

# An Alternative Lattice Design for ILC Damping Ring\*

SUN Yi-Peng<sup>1,2;1)</sup> GAO Jie<sup>2</sup> GUO Zhi-Yu<sup>1</sup>

1 (Key Laboratory of Heavy Ion Physics, Ministry of Education & School of Physics,  
Peking University, Beijing 100871, China)

2 (Institute of High Energy Physics, CAS, Beijing 100049, China)

**Abstract** The ILC damping rings should provide beams with very low natural emittances for the linear collider to reach the required luminosity, and at the same time, the damping rings also need to have a large acceptance to ensure good injection efficiency for high emittance, high energy spread beam from the positron source. Meeting the above requirements is a real challenge for the ILC damping ring lattice design. In order to reduce the cost for ILC damping rings, an alternative lattice different from the baseline configuration design has been done with modified FODO cells, and the total quadrupole number has been reduced by half. The new lattice has been optimised to have good dynamic apertures.

**Key words** ILC, damping ring, FODO cell, lattice, dynamic aperture

## 1 Introduction

The International Linear Collider (ILC) which is based on superconducting RF acceleration technology requires the damping rings to provide beams with extremely small equilibrium emittances, and large acceptance<sup>[1]</sup>. Another main design criteria for the damping ring comes from the requirement of providing a long beam pulse of 1ms containing 2820 bunches (normal parameter set<sup>[2]</sup>), corresponding to an approximately 300km long bunch train. To keep the damping ring's circumference reasonable, the bunch train has to be stored in a compressed mode with much smaller bunch spacing than in the linacs. Consequently, each bunch has to be individually injected and ejected. The ring circumference is then determined both by pulse width of the injection and extraction kicker system and electron-cloud (ion) effects. Based on the studies of the various configuration options, the ILC damping ring Baseline Configuration Design (BCD) decides that the positron

damping ring should consist of two (roughly circular) rings of approximately 6km circumference in a single tunnel and the electron damping ring should consist of a single 6km ring, assuming that the fill pattern allows a sufficient gap for clearing ions<sup>[2, 3]</sup>, and the basic requirements of the positron damping ring design which is shown in Table 1.

Table 1. Beam parameters for positron ring.

injected emittance $\gamma\varepsilon_{x(y)}$	0.01m-rad
extracted emittance $\gamma\varepsilon_x/\gamma\varepsilon_y$	$8 \times 10^{-6}/2 \times 10^{-8}$ m-rad
damping time	28ms
pulse length	1ms
number of bunches	2820
particles per bunch	$2 \times 10^{10}$

In the ILC damping ring baseline design, a lattice of circumference of  $\sim 6$ km using TME arc cells has been used<sup>[4]</sup>. In this paper, with the aim to reduce the cost of the damping rings, a new lattice with modified FODO arc cells is designed to be an alternative of the baseline design.

In the following sections, the linear lattice design, the chromaticity correction, and the optimisation of

Received 21 June 2006

\* Supported by National Natural Science Foundation of China (10525525)

1) E-mail: ypsun@mail.ihep.ac.cn

the dynamic aperture will be presented.

## 2 The linear lattice design

### 2.1 The arc cell

There are 120 arc cells in all for a 6km damping ring, therefore each arc cell provides a bending angle of  $\pi/60$  for the beam. The FODO arc cell length is selected as 38.9m and the phase advance per arc cell is  $90^\circ/90^\circ$  for the horizontal and vertical betatron motion, respectively. According to Eq. (1), the maximum and the minimum value of the beta functions of the FODO arc cell is 66.2m and 11.4m, respectively. From Eq. (2), the maximum and the minimum horizontal dispersion function is 1.37m and 1.02m, respectively which are too large to get a reasonable bunch length of 6mm.

$$\beta^\pm = \frac{L_P \left(1 \pm \sin \frac{\mu}{2}\right)}{\sin \mu}, \quad (1)$$

$$D^\pm = \frac{L_P \phi \left(1 \pm \frac{1}{2} \sin \frac{\mu}{2}\right)}{4 \sin^2 \frac{\mu}{2}}, \quad (2)$$

where  $\beta^+$  and  $\beta^-$  are the maximum and minimum value of the beta functions,  $D^+$  and  $D^-$  are the maximum and minimum value of the horizontal dispersion function,  $L_P$  is the length of the cell,  $\mu$  is the phase advance of the cell, and  $\phi$  is the bending angle in one arc cell. To have smaller rms dispersion value, the length of the drifts that are between the quadrupoles is adjusted and the ultimate value of the two long drifts are 13.7m and 1.55m with the maximum and the rms horizontal dispersion function being 1.15m and 0.77m, respectively.

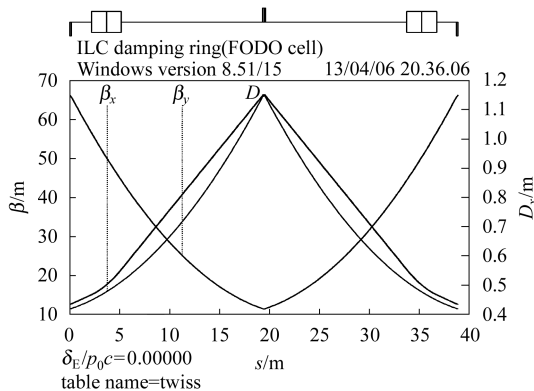


Fig. 1. Lattice functions in an arc cell.

The lattice functions in an arc cell are shown in Fig. 1 and the main parameters of the arc cell are shown in Table 2.

Table 2. Main parameters of the arc cell.

cell length	38.9m
max/min beta functions	66.1m/11.4m
max/RMS dispersion	1.15m/0.77m
phase advance $x/y$	0.25/0.25

### 2.2 The RF and wiggler cell

The vertical damping time can be written as follows:

$$\tau_y = \frac{3C}{r_e c \gamma^3 I_2} = \frac{3C}{r_e c \gamma^3 (I_{2a} + I_{2w})}, \quad (3)$$

where  $C$  is the circumference,  $r_e$  is the classical electron radius,  $c$  is the speed of light,  $\gamma$  is the normalized beam energy, and  $I_2$  is the second synchrotron integral over dipoles and wigglers.

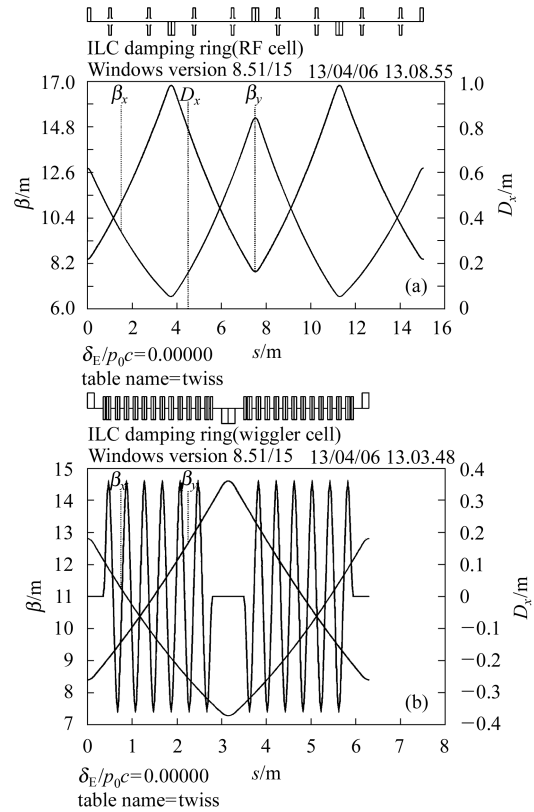


Fig. 2. Lattice functions in RF (a) and wiggler cell(b).

The equilibrium horizontal emittance can be written as:

$$\gamma \varepsilon_x = \frac{C_q \gamma^3 I_5}{J_x I_2}, \quad (4)$$

where  $C_q \approx 3.84 \times 10^{-13} \text{m}$ ,  $J_x \approx 1$  for separate function magnet, and  $I_5$  is determined by the arc sections.

The wiggler section is designed to provide enough damping. The average beta functions in this section are about 10m, and totally 40 such wiggler sections have been used for positron damping ring. The lattice functions in a RF cell and in a wiggler cell are shown in Fig. 2.

### 2.3 The long straight sections

There are two long straight sections which are designed to be dispersion free. One is designed for the injection and the extraction of the beam. The incoming electrons (or positrons) are injected into the empty RF buckets in the ring, rather than being added to the contents of bunches already orbiting the ring. In addition, the emittance of an incoming positron bunch is very large. As a result, the injection and extraction optics must be designed to accommodate these beam characteristics while still achieving high injection and extraction efficiencies.

The injection and extraction optics are designed to accommodate either of two different types of kickers that are studied at Fermilab : a pulsed kicker system with 6ns rise time (and longer fall time) and a Fourier kicker, which is shown in Fig. 3.

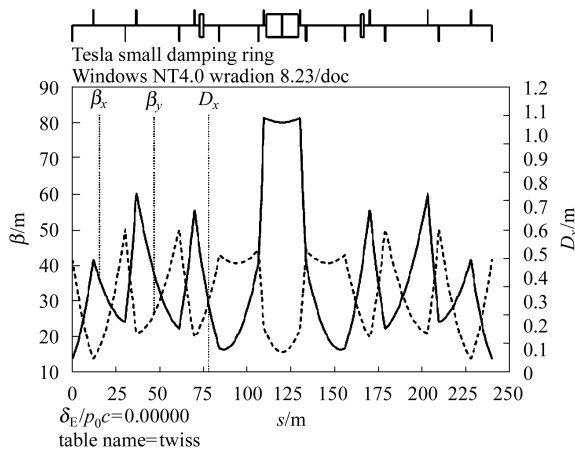


Fig. 3. The injection and extraction optics.

As for the other long straight section, it should be stressed that it can be changed to give a proper phase advance which plays a dominant role in the optimization of the dynamic aperture.

### 2.4 The dispersion suppressors

These insertions match the dispersion function between arc sections and straight sections. There are

two kinds of dispersion suppressor insertions. One kind matches dispersion without affecting the alpha and beta functions, and the other suppresses the dispersion function by only modifying the focal length of two quadrupoles, which modifies both the alpha and beta functions.

Here we do not use the usual method to make a dispersion suppressor, but insert three quadrupoles into the arc cell to get a dispersion suppressor, as shown in Fig. 4.

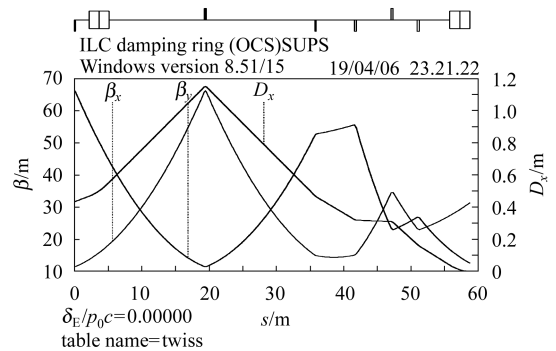


Fig. 4. Lattice functions in a dispersion suppressor.

### 2.5 The whole ring

The layout of the ring has been designed with two-fold symmetry. There are totally ten long straight sections. The RF cavity and the wigglers have been installed in eight of them. The other two long straight sections are designed to accommodate various injection and extraction schemes, also used to adjust the phase advance.

The lattice functions for the whole ring are shown in Fig. 5 and the principal lattice parameters are listed in Table 3.

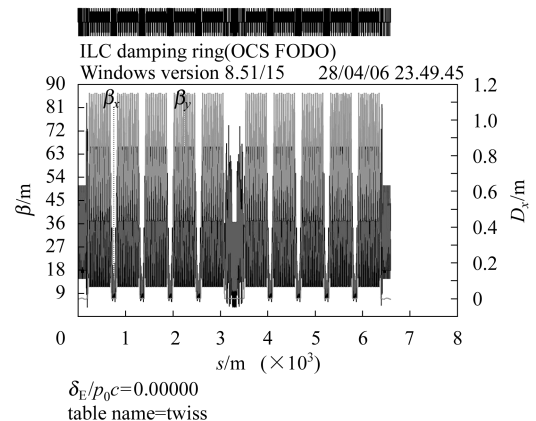


Fig. 5. Lattice functions for the whole ring.

Table 3. The principle lattice parameters.

circumference/m	6614.057
energy/GeV	5
arc cell	FODO
tune	53.6368/48.7552
natural chromaticity	-65.1/-65.3
momentum compaction( $10^{-4}$ )	4.11
transverse damping time/ms	25/25
Norm. natural emittance/(mm·mrad)	4.2
RF voltage/MV	46.6
synchrotron tune	0.093
synchrotron phase/( $^{\circ}$ )	169.2
RF frequency/MHz	650
RF acceptance/(%)	2.68
natural bunch length/mm	5.96
natural energy spread/( $10^{-3}$ )	1.28

### 3 Chromaticity correction

#### 3.1 Chromaticity correction and DA

Two family sextupoles in the arc cell are used to correct the first order chromaticity to zero. The phase advance per arc cell is  $90^{\circ}/90^{\circ}$  for the horizontal and vertical betatron motion, respectively. There are totally ten arc sections and twelve arc cells in each arc section. Therefore, the phase advance per arc section is  $3\pi$  for both the horizontal and vertical motion. This kind of second order achromat helps to cancel all driving terms of the third order resonances generated by the sextupoles within each arc section.

The phase advance between the arc sections, that is to say in the straight sections, also plays a dominant role in determining the dynamic aperture. Roughly, it is thought that the best phase advance in the straight section is nearly a multiple of  $360^{\circ}$ , which makes the whole straight section an identity transformation and therefore maximizes the symmetry of the ring and minimizes the number of excited high order resonances<sup>[5]</sup>.

In our study it is found that not only the phase advance in the straight section but also between the last sextupole in one arc section and the first sextupole in the next arc section are very important. The straight sections are optimized to give a reasonable horizontal phase advance which is near  $2\pi$ , and a vertical phase advance which is near  $\pi$ .

The position of the two family sextupoles in the

arc cell has been adjusted to give a good chromaticity property and a larger dynamic aperture. The variation of tune with momentum spread  $\pm 1\%$  is shown in Fig. 6(a). After tracking for 512 turns, the dynamic aperture of both on-momentum and off-momentum particles is obtained, which is shown in Fig. 6(b)<sup>[6]</sup>.

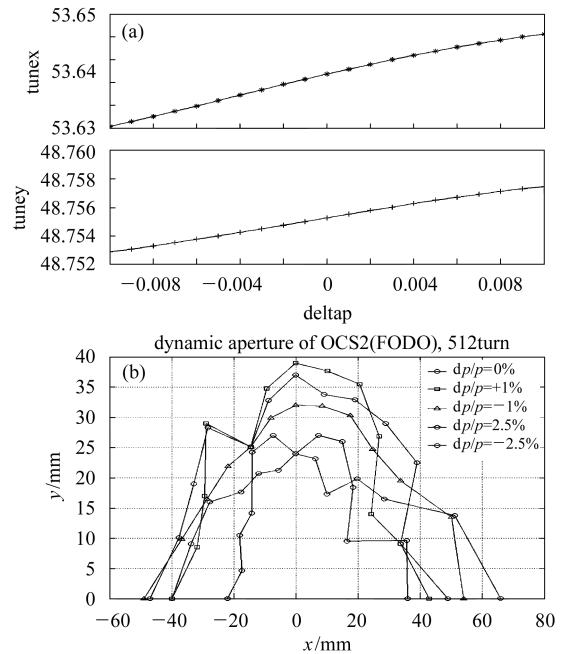


Fig. 6. The tune variation with momentum spread  $\pm 1\%$  (a); the dynamic aperture with momentum spread up to  $\pm 2.5\%$  (b).

It can be calculated from the injected beam's emittance and the beta functions at the injection point of the ring that the horizontal and vertical bunch sizes of the injected beam are approximately 6.6mm and 4.2mm, respectively. It can be seen from Fig. 5(b) that the dynamic aperture is ten times the vertical injected beam size and eight times the horizontal injected beam size for on momentum particles, and the lattice also gives a good dynamic aperture for off momentum particles.

As the nonlinear wiggler effect is not included in the tracking process, we use analytical method to calculate the dynamic aperture of the damping ring with ideal nonlinear wigglers<sup>[7]</sup>. One has the dynamic aperture limited by one wiggler as follows (vertical and horizontal respectively):

$$A_{N_w,y}(s) = \sqrt{\frac{3\beta_y(s)}{\beta_{y,m}^2}} \frac{\rho_w}{k_y \sqrt{L_w}}, \quad (5)$$

$$A_{N_w,x}(s) = \sqrt{\frac{\beta_y(s)}{\beta_x(s)} (A_{N_w,y}^2(s) - y^2)}, \quad (6)$$

where  $\beta_y(s)$  and  $\beta_x(s)$  are the unperturbed beta functions,  $\beta_{y,m}$  is the vertical beta function at the middle of the wiggler,  $\rho_w$  is the radius of curvature of the wiggler peak magnetic field  $B_0$ ,  $L_w = N_w \lambda_w$  is the wiggler length,  $k_y = 2\pi/\lambda_w$ ,  $\lambda_w$  is the period length of the wiggler, and  $N_w$  is the cell number of a wiggler.

Assuming that the dynamic aperture of the ring without the wiggler's effects is  $A_y$  and that there are  $M$  wigglers to be inserted inside the ring at different places, one has the total dynamic aperture expressed as:

$$A_{\text{total},y}(s) = \frac{1}{\sqrt{\frac{1}{A_y(s)^2} + \sum_{j=1}^M \frac{1}{A_{j,w,y}(s)^2}}}, \quad (7)$$

where  $A_{j,w,y}$  denotes the dynamic aperture limited by the  $j$ -th wiggler.

Using Eqs. (5), (6) and (7), the dynamic aperture of both on-momentum and off-momentum particles which includes nonlinear wiggler effects is shown in Table 4, where off-momentum particles' dynamic aperture is also calculated.  $A_{y0}$  and  $A_{x0}$  are the vertical and horizontal dynamic apertures with linear wiggler model.  $A_y$  and  $A_x$  are the corresponding vertical and horizontal dynamic apertures including nonlinear wiggler effects.

Table 4. DA using nonlinear wiggler.

$\Delta P/P$	$A_y/\text{mm}$	$A_x/\text{mm}$	$A_{y0}/\text{mm}$	$A_{x0}/\text{mm}$
0	25	39.5	38	50
-1%	22.8	36	34	48
$\pm 2.5\%$	21	33.18	28	36

It can be seen from Table 4 that the dynamic aperture of the designed damping ring, where nonlinear wiggler effect has been taken into account, is greater than six times the injected beam size for on momentum particles and five times the injected beam size for off momentum particles.

### 3.2 FMA analysis

Frequency map analysis (FMA) is introduced for the demonstration and understanding of the chaotic behavior of a dynamical system. The application to

particle accelerator dynamics is done in the case that the motion of a single particle in a storage ring is described in a surface of section of the beam by a symplectic map of dimension 4 or 6<sup>[8]</sup>.

Here FMA is used to optimize the working points and the dynamic aperture. The optimized result is shown in Fig. 7 where 2500 particles distributed at the range of seven times the injected bunch size are tracked for 1024 turns to do the frequency map analysis on the lattice.

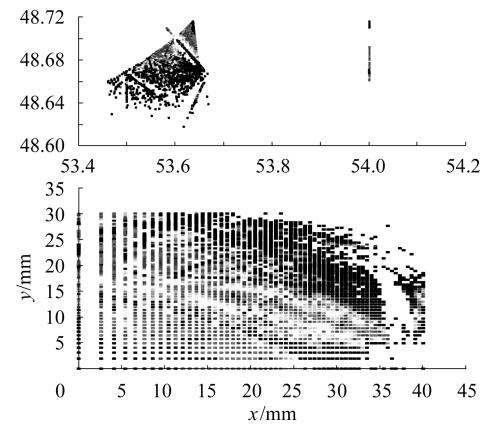


Fig. 7. FMA analysis for damping ring DA.

## 4 Conclusions

To reduce the ILC damping ring cost, an alternative lattice with modified FODO cells has been designed. The number of quadrupoles in the whole ring has been decreased by half compared with the original ILC damping ring BCD design. The equilibrium emittances, bunch length, acceptance, dynamic apertures, and the damping time can fulfill the requirements for the ILC damping ring. The dynamic aperture is large enough including the nonlinear wiggler effects and it can be optimized further by adjusting the phase advance of the long straight section. Frequency map analysis has been used on this lattice during the optimization of the dynamic apertures by choosing the working point far away from the dangerous resonance line, and the result shows that the lattice can be further optimized.

*The author would like to thank XU Gang, QIN Qing, JIAO Yi and other colleagues in the physics group for their helpful discussions.*

## References

- 1 GAO J. HEP & NP, 2006, **30**(Supp. I): 156(in Chinese)  
(高杰. 高能物理与核物理, 2006, **30**(增刊 I): 156)
- 2 Wolski A, GAO J, Guiducci S. EPAC06. 2006
- 3 ILC BCD. <http://www.linearcollider.org/>
- 4 XIAO A. <http://www.desy.de/~awolski/ILCDR>
- 5 CAI Y. SLAC-PUB-11084
- 6 AT User's Manual. SLAC-PUB 8732
- 7 GAO J. Nucl. Instrum. Methods, 2000, **A451**(3): 545
- 8 Dumas S, Laskar J. Phys. Rev. Lett., 1993, **70**: 2975

## 国际未来直线对撞机(ILC)阻尼环 Lattice 设计\*

孙一鹏<sup>1,2;1)</sup> 高杰<sup>2</sup> 郭之虞<sup>1</sup>

1 (北京大学重离子物理研究所 北京 100871)

2 (中国科学院高能物理研究所 北京 100049)

**摘要** 为了使国际未来直线对撞机达到高的亮度,对撞机的阻尼环必须要有很小的自然发射度.同时,阻尼环要有很大的接收度来接受来自正电子注入系统的大能散、大发射度的正电子束团.对于磁聚焦结构的设计来说,同时达到以上要求是一件很有挑战性的工作.为了降低ILC阻尼环的造价采用修正的FODO结构设计了可以满足ILC要求的阻尼环备用Lattice,并使四极磁铁的数量比起ILC阻尼环BCD设计减少了一半.

**关键词** 国际未来直线对撞机(ILC) 阻尼环 FODO结构 磁聚焦结构 动力学孔径